JB
Journals.ASM.org

Aconitase-Mediated Posttranscriptional Regulation of *Helicobacter pylori* Peptidoglycan Deacetylase

Crystal M. Austin, Robert J. Maier

Department of Microbiology, University of Georgia, Athens, Georgia, USA

Some bacterial aconitases are bifunctional proteins that function in the citric acid cycle and act as posttranscriptional regulators in response to iron levels and oxidative stress. We explore the role of aconitase (AcnB) in *Helicobacter pylori* as a posttranscriptional regulator of the cell wall-modifying enzyme peptidoglycan deacetylase, PgdA. Under oxidative stress, PgdA is highly expressed and confers resistance to lysozyme in wild-type cells. PgdA protein expression as well as transcript abundance is significantly decreased in an *acnB* mutant. In the wild type, *pgdA* mRNA half-life was 13 min, whereas the half-life for the *acnB* strain was 7 min. Based on electrophoretic mobility shift assays and RNA footprinting, the *H. pylori* apo-AcnB binds to the 3′-untranslated region of the *pgdA* RNA transcript. Some of the protected bases (from footprinting) were localized in proposed stem-loop structures. AcnB-*pgdA* transcript binding was abolished by the addition of iron. The *acnB* strain is more susceptible to lysozyme-mediated killing and was attenuated in its ability to colonize mice. The results support a model whereby apo-AcnB directly interacts with the *pgdA* transcript to enhance stability and increase deacetylase enzyme expression, which impacts *in vivo* survival.

Helicobacter pylori is a Gram-negative, microaerophilic bacterium that infects over 50% of the world's population and is the etiological agent for gastritis, peptic ulcer disease, and most gastric cancers (1). During colonization of the human gastric mucosa, *H. pylori* induces a strong inflammatory response resulting in the production of large amounts of reactive oxygen species (ROS). *H. pylori* can thrive in the gastric mucosa by employing a battery of diverse antioxidant enzymes that detoxify oxidants and repair essential biomolecules (2, 3). Additionally, *H. pylori* utilizes other mechanisms to persist in the host, including peptidoglycan (PG) modification (4).

H. pylori PG consists of alternating *N*-acetylglucosamine (GlcNAc) and *N*-acetylmuramic acid (MurNAc) residues connected by β-1,4 bonds and cross-linked via short peptide bridges (5, 6). The β-1,4 bonds are susceptible to hydrolysis by the muramidase lysozyme, which results in decreased cell wall integrity and cell lysis. Lysozyme, an important component of the host innate immune system, is abundant in the mucosal surface and is present in the granules of professional phagocytes (7, 8). Interestingly, bacteria have evolved mechanisms to modify their PG around the lysozyme cleavage site to prevent hydrolysis (9). *H. pylori* is equipped with a peptidoglycan deacetylase (PgdA) that confers both pure PG and whole bacterial resistance to lysozyme degradation (10). PgdA expression is significantly increased in *H. pylori* cells when they are exposed to oxidative stress and when in contact with macrophages (10, 11). Furthermore, *pgdA* mutants have an attenuated ability to colonize the mouse stomach and permit a stronger host immune (cytokine) response (11). This previous work led us to question how PgdA expression is regulated, especially considering that *H. pylori* lacks many of the oxidative stress response regulators found in most other Gram-negative bacteria. We hypothesized that aconitase plays an important role during oxidative stress by serving as a posttranscriptional regulator for peptidoglycan deacetylase (10).

Aconitases are [4Fe-4S] proteins that catalyze the reversible isomerization of citrate to isocitrate in the citric acid cycle. In eukaryotes, there are two types of aconitase proteins, mitochondrial aconitase (m-Acn) and cytosolic aconitase (c-Acn), also referred to as iron regulatory protein 1 (IRP1). IRP1 is bifunctional, having enzymatic activity when the [4Fe-4S] cluster is intact and acting as a posttranscriptional regulator when the cluster is disassembled (12). Iron deprivation and oxidative stress are known to cause disassembly of the cluster, resulting in the apo-form of IRP1, which undergoes domain rearrangements that allow it to bind to iron-responsive elements (IREs) (12, 13). IREs are approximately 30-nt-long sequences that form stem-loop structures in the untranslated regions (UTRs) of mRNA transcripts. The eukaryotic consensus IRE contains a C bulge in the stem and the sequence CAGUGN in the loop (14). If the IRE is located in the 5′ UTR, binding of IRP1 will inhibit translation; if the IRE is located in the 3′ UTR, binding of IRP1 will increase transcript stability and result in enhanced translation (12, 14).

Several bifunctional bacterial aconitases have been studied thus far, including *Escherichia coli* AcnA and AcnB, which have been found to enhance and decrease superoxide dismutase (SodA) expression, respectively (15). In *Salmonella enterica* serovar Typhimurium LT2, AcnB was shown to indirectly regulate the flagellum protein, FliC (16). *Bacillus subtilis* aconitase (CitB) binds to the 3′ UTR of *gerE*, a transcriptional activator and repressor involved in sporulation (17). Furthermore, *Mycobacterium tuberculosis* aconitase (Acn) binds to the thioredoxin (*trxC*) transcript and to the *ideR* transcript, an iron-dependent activator and repressor (18). *H. pylori* possesses one copy of aconitase, *acnB*, whose gene product is known to have aconitase activity in the citric acid cycle (19), but it has not yet been studied as a posttranscriptional regulator. Here, we present evidence that apo-AcnB acts as a posttranscriptional regulator for PgdA, which is an im-

Received 22 June 2013 **Accepted** 18 September 2013
Published ahead of print 20 September 2013
Address correspondence to Robert J. Maier, rmaier@uga.edu.

doi:10.1128/JB.00720-13

portant PG modification enzyme conferring lysozyme resistance, and that it contributes to survival in the mouse host.

MATERIALS AND METHODS

Bacterial strains and growth conditions. *H. pylori* X47 and 43504 wild-type and *acnB* strains were grown on Brucella agar (Difco) supplemented with 10% defibrinated sheep blood (BA plates) and chloramphenicol (50 μg/ml) at 37°C under constant microaerophilic conditions (2% O_2). For mRNA half-life determinations, wild-type and mutant strains were grown in brain heart infusion (BHI) broth with 0.4% β-cyclodextrin. Sealed bottles initially contained 5% CO_2, 10% H_2, 75% N_2, and 10% O_2 and were incubated at 37°C with shaking. The *H. pylori* wild-type and *acnB* strain growth patterns were similar. *E. coli* BL21 RIL cells were grown at 37°C aerobically on Luria-Bertani agar or broth (shaking) supplemented with ampicillin (100 μg/ml) and chloramphenicol (50 μg/ml).

Mutant construction. The 2.6-kb *acnB* gene (*hp0779*) has been determined to be the first gene of an operon containing 3 additional genes: *hp0780*, *hp0781*, and *hp0782* (20). Ninety-eight percent of the gene was deleted from *H. pylori* strains X47 and 43504 using overlap extension PCR and was replaced with the chloramphenicol (*cat*) cassette, which was inserted in the same direction of transcription as that of the native gene. The *cat* cassette has its own promoter, lacks a transcription terminator, and is routinely used in our laboratory without any polar effect (21, 22). Primers acnB1 (5′-CCCCGCATCAATACGCC-3′) and acnB2 (5′-ATCCACTTTTCAATCTATATCCTAAAAAATCTTTCATCAT-3′) were used to amplify a 327-bp DNA sequence that contained the beginning of *hp0778*, the intergenic region between *hp0778* and *hp0779*, the beginning of *hp0779*, and a portion of the *cat* cassette. Primers acnB3 (5′-CCCAGTTTGTCGCACTGATAAGGAGAATTTCAGGCTCTAG-3′) and acnB4 (5′-CTAGCGCCAATTATAGATATAAGG-3′) were used to amplify a 388-bp sequence containing part of the *cat* cassette, the end of *hp0779*, the intergenic region between *hp0779* and *hp0780*, and *hp0780*. Primers acnB1 and acnB4 were used in the final PCR step to fuse together the product of acnB1/acnB2, the *cat* cassette, and the product of acnB3/acnB4. This final step yielded a 1.5-kb PCR product that was then cloned into the pGEM-T vector (Promega) to generate pGEM*acnB*::*cat*. This plasmid was introduced into the wild-type strain via natural transformation and homologous recombination. *acnB* mutants were selected on BA plates with chloramphenicol (50 μg/ml) at 2% O_2. Insertion of the *cat* cassette and absence of the *acnB* gene were confirmed by PCR and sequencing using primers acnB1 and acnB4 and primers specific for the *cat* cassette (5′-GATATAGATTGAAAAGTGGAT-3′ and 5′-TTATCAGTGCGACAAACTGGG-3′). Also, reverse transcription-PCR (RT-PCR) was performed on the downstream gene, *hp0781*, to rule out a possible polar effect due to the *cat* cassette. Since *hp0780* is only 273 bp in length, we instead designed primers for *hp0781* (1.3 kb). Total RNA was extracted (Aurum total RNA mini kit; Bio-Rad), treated with DNase (Turbo DNA-free kit; Ambion), and used as a template for cDNA synthesis (iScript cDNA synthesis kit; Bio-Rad). The generated cDNA was then used as a template for PCR, and a product of the expected size was obtained for both the wild-type and *acnB* strains (data not shown).

Western blotting. *H. pylori* wild-type and *acnB* strains were each separately grown under 2% O_2 for 36 h and 12% O_2 for 72 h. The time for cells grown under 12% O_2 was extended, because cell growth is slower at this higher oxygen level. Cell extracts were subjected to SDS-PAGE, and the proteins were electroblotted onto a nitrocellulose membrane. The membrane was then incubated with anti-PgdA (1:500) (Antagene, Inc.) followed by exposure to goat anti-rabbit IgG alkaline phosphatase-conjugated secondary antibody (1:1,000) (Bio-Rad). Anti-UreA (1:10,000) (Santa Cruz Biotechnology) was used as an internal loading control. ImageJ (http://rsbweb.nih.gov/ij/) was used to analyze dried membranes. Student's *t* test was used for statistical comparisons.

Real-time quantitative PCR. The Aurum total RNA mini kit (Bio-Rad) was used to extract total RNA from *H. pylori* wild-type and *acnB* cells grown under 2 and 12% O_2. The Turbo DNA-free kit (Ambion) was used as an additional measure to degrade any remaining DNA. cDNA was synthesized using the iScript cDNA synthesis kit (Bio-Rad) according to the kit instructions. The iQ SYBR green supermix (Bio-Rad) kit was used for real-time PCR according to the manufacturer's protocol. Primers specific for *pgdA* (5′-GGATTCGCCTGATGATATTTCG-3′ and 5′-CCTGCATCCACGATCATTTTC-3′) were used along with primers specific for *gyrA* (5′-GCTAGGATCGTGGGTGATGT-3′ and 5′-TGGCTTCAGTGTAACGCATC-3′), the internal control. Relative transcript abundance was calculated using the $2^{-\Delta CT}$ formula (23). For mRNA half-life determinations, wild-type and *acnB* strains were grown in BHI for 24 h (early exponential phase) and subjected to 21% O_2 for 2 h. Rifampin (500 μg/ml) was added, and after 70 s ($t = 0$) time points were established (2, 5, 10, 15, 20, and 30 min). For each time point, RNA was extracted as described above and cDNA was synthesized using primers specific for *pgdA*. The quantitative PCR (qPCR) data were used to calculate the *pgdA* mRNA half-life as described previously (24). Prism (GraphPad, San Diego, CA) was used with the equation $Y = (Y_0)e^{-kt}$, where Y is the percent *pgdA* mRNA remaining at time t, to find first-order decay constants (k) by nonlinear regression analysis. Half-lives were calculated using $t_{1/2} = \ln 2/k$ (24).

Overexpression and purification of AcnB. The *H. pylori acnB* gene was PCR amplified using wild-type DNA as the template with primers acnBHisF (5′-CGCACCCATATGATGAAAGATTTTTTAGAAG-3′) and acnBHisR (5′-GAAGACCTCGAGGAGCCTGAAATTCTCCATTAAG-3′). The PCR product was cloned into the pET-21b vector (Novagen) and overexpressed as a hexahistidine-tagged protein in *E. coli* BL21 RIL. Cells were grown in LB broth to an A_{600} of 0.5 and induced with 0.5 mM isopropyl β-D-1-thiogalactopyranoside for 4 h. After harvesting by centrifugation (5,000 × *g*, 10 min, 4°C) and resuspending and washing the pellet with 50 mM NaH_2PO_4, 300 mM NaCl, pH 8 (buffer A supplemented with 10 mM imidazole), cells were resuspended in the same buffer and lysed by three passages though a French pressure cell (22). Following centrifugation of the extract (16,000 × *g*, 30 min), the supernatant was collected and applied to a nickel-nitrilotriacetic acid column (Qiagen). The column was washed with buffer A supplemented with 20 mM imidazole, and the protein was eluted with buffer A supplemented with 250 mM imidazole. Purified protein was analyzed by SDS-PAGE and estimated to be approximately 95% pure. Apo-AcnB was prepared by incubating the purified native protein with dipyridyl (0.5 mM) for 30 min and then dialyzing overnight against 20 mM Tris-Cl, pH 8, 100 mM NaCl, 3% glycerol (18). As expected, the UV-visible absorption spectrum of native AcnB showed absorbance in the 300- to 600-nm range indicative of Fe-S clusters, while absorbance in this range was significantly lower for the dipyridyl-treated protein (data not shown). Protein concentration was determined using the bicinchoninic acid assay kit (Thermo Scientific).

Electrophoretic mobility shift assays. The entire *pgdA* mRNA 3′ UTR (45 nt) was synthesized (Integrated DNA Technologies) and radiolabeled at the 5′ end with T4 polynucleotide kinase (Invitrogen) according to the manufacturer's instructions. A 2.5-μl sample of [γ-^{32}P]ATP (10 μCi/μl; 3,000 Ci/mmol) was incubated with 5 pmol of *pgdA* RNA, 1× forward reaction buffer, T4 polynucleotide kinase, and water for 10 min at 37°C. Labeled RNA was purified by phenol extraction and ethanol precipitation. Size and purity were checked on a denaturing urea polyacrylamide gel. Purified *pgdA* RNA (50 nM) was incubated with either increasing apo-AcnB (0, 600, 1,200, and 3,000 nM) or bovine serum albumin (BSA) (3,000 nM) in binding buffer (10 mM Tris pH 8.3, 20 mM KCl, and 10% glycerol) with 130-fold nonspecific yeast tRNA for 15 min at room temperature. Apo-AcnB (3,000 nM) was incubated with either 1 mM ammonium iron (II) sulfate plus 10 mM dithiothreitol or 0.5 mM dipyridyl. Unlabeled specific *pgdA* competitor (50× and 100× molar excess) was added to apo-AcnB (3,000 nM) in some reactions prior to the addition of radiolabeled *pgdA* RNA and allowed to incubate for 5 min to maximize effectiveness (recommended by Thermo Scientific). As a positive control for the binding reactions, the 5′ UTR human ferritin sequence (5′-GTGAGAGAATTCGGGAGAGGATTTCCTGCTTCAACAGTGCTTGGACGGAACTTTGTCTTGAAGCTTGGAGAG-3′) was synthesized (Integrated

DNA Technologies) and cloned into the pGEM-3Z vector (Promega). HindII was used to generate the linearized plasmid, which was then used as a template for *in vitro* transcription. T7 RNA polymerase (Promega) was used to synthesize radiolabeled RNA using [α-^{32}P]UTP (10 μCi/μl; 800 Ci/mmol) according to the manufacturer's instructions. RNA was purified by phenol extraction and ethanol precipitation. As a negative control, the pGEM-3Z vector alone was linearized and subjected to *in vitro* transcription. The positive- and negative-control reactions were performed using 3,000 nM apo-AcnB. Reaction products were resolved on a 6% nondenaturing polyacrylamide gel. The gel was incubated overnight in a phosphor screen cassette (Molecular Dynamics), and the screen was scanned using the Typhoon Imager (GE Healthcare).

RNA footprinting. 5′-End-labeled *pgdA* probe was prepared as described for electrophoretic mobility shift assays. *pgdA* probe (50 nM) was incubated for 15 min at room temperature with (1 μM) and without apo-AcnB, 1× RNA structure buffer (Ambion), 1 μg of yeast tRNA, and either RNase A (1 ng) or RNase V_1 (0.001 U). Digestion products were purified by phenol extraction and ethanol precipitation. Samples were resolved on a 20% denaturing polyacrylamide 7 M urea gel in 1× Tris-borate-EDTA (TBE). The gel was vacuum dried, incubated overnight in a phosphor screen cassette (Molecular Dynamics), and scanned using a Typhoon imager (GE Healthcare).

Lysozyme sensitivity assays. Wild-type and *acnB* strains were grown to late exponential phase under microaerophilic conditions, harvested, resuspended in phosphate-buffered saline (PBS) to an optical density at 600 nm (OD_{600}) of 1, and then subjected to incubation for 8 h with lysozyme (50 mg/ml). After incubation, cells were serially diluted and plated, and colonies were counted after 4 days. Significant differences between the wild type and mutant were determined using Student's *t* test.

Mouse colonization. All procedural work was approved by the Institutional Animal Care and Use Committee at the University of Georgia, Athens, GA. *H. pylori* wild-type and *acnB* strains were grown on BA plates under microaerophilic conditions for 48 h. Cells were suspended in PBS to an OD_{600} of 1.7, and 3×10^8 cells were administered to each C57BL/6J mouse. Three weeks after inoculation, the mice were sacrificed after withholding food and water for 1.5 to 2 h and the stomachs were removed, weighed, and homogenized. Stomach homogenate dilutions were made in PBS and plated onto BA plates supplemented with amphotericin B (10 μg/ml), bacitracin (100 μg/ml), and vancomycin (10 μg/ml). After 5 days of incubation under microaerophilic conditions, cells were enumerated and the data expressed as log(CFU/g) of stomach. The Wilcoxon signed-rank test was used to determine significant differences in colonization between the wild-type and mutant strains.

RESULTS

PgdA expression, transcript abundance, and mRNA half-life in the strains upon oxidative stress exposure. We began this work by investigating the effect of the aconitase deletion on expression of peptidoglycan deacetylase (PgdA). Western blot analyses were performed using anti-PgdA antibody and cell extracts from wild-type and *acnB* strains grown under both 2% O_2 for 36 h and 12% O_2 for 72 h. A significant difference in PgdA expression was found for the wild type at 2 versus 12% O_2 (Fig. 1), similar to the previous finding that reported PgdA is increased upon subjection of cells to oxidative stress (10). No significant difference in PgdA levels was found in the *acnB* mutant between 2 and 12% O_2. There was a decrease in PgdA expression in the *acnB* strain under 2% O_2 compared to the wild type under the same condition. Interestingly, there was 4-fold less PgdA expression in the *acnB* strain under 12% O_2 compared to the wild type under 12% O_2.

pgdA transcript abundance was assessed in the *acnB* strain using quantitative real-time PCR (Fig. 2). Wild-type and *acnB* strains were subjected to the same growth conditions as those

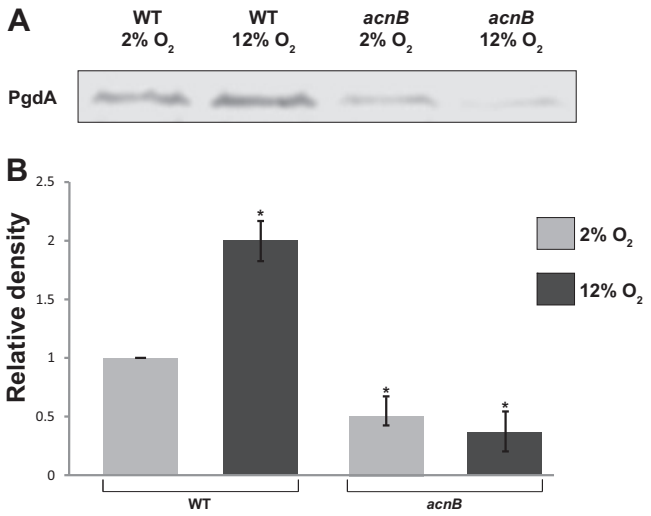

FIG 1 Expression of the PgdA enzyme at two oxygen levels. Western blot (A) and (B) densitometry analysis of PgdA expression from the Western blot are shown. Cell extracts from 43504 wild-type and *acnB* strains were subjected to SDS-PAGE followed by immunoblotting using specific anti-PgdA antibody. Dried blots were analyzed using ImageJ. Wild-type (2% O_2) expression was used as the reference (adjusted to 1.0 U). The experiment included an internal loading control, UreA (not shown), that verified equal amounts of protein were loaded. Data shown are averages and standard deviations (SD) from three independent experiments. Asterisks indicate a significant difference compared to the reference. $P < 0.01$ as determined by Student's *t* test.

described for the Western blot experiments. There was a 2-fold increase in relative *pgdA* transcript abundance for the wild type under 12% O_2 compared to the 2% O_2 condition, which was expected. *pgdA* transcript levels in the *acnB* mutant under 12% O_2 were 2-fold decreased compared to those at the 2% O_2 incubation. A 3-fold decrease in *pgdA* abundance was found in the *acnB* strain under 2% O_2 versus the wild type under the same condition. Most interestingly, a 9-fold decrease was observed for the *pgdA* transcript in the *acnB* strain under 12% O_2 versus the wild type under 12% O_2.

To directly determine if AcnB was functioning as a posttranscriptional regulator to stabilize the *pgdA* message, we used qPCR to calculate the half-life of the *pgdA* mRNA in the wild-type and *acnB* strains. Cells were grown under microaerophilic conditions and then exposed to 21% O_2 for 2 h. Our results revealed that upon high oxygen exposure, the wild-type *pgdA* mRNA half-life is 13 min, whereas the *acnB* mutant *pgdA* mRNA half-life is 7 min.

In summary, these findings suggested that apo-AcnB directly interacts with the *pgdA* transcript. The model is that under oxidative stress, the [4Fe-4S] cluster of AcnB is likely to be disassembled and apo-AcnB binds to the *pgdA* transcript, stabilizing the message and resulting in increased transcript abundance and expression.

Apo-AcnB binds to the *pgdA* 3′ UTR. Since it is known that aconitase can function as a posttranscriptional regulator and the results described above suggested aconitase was interacting with the *pgdA* transcript, we examined the 5′ and 3′ UTRs of the *pgdA* gene for possible IRE-like sequences. The *pgdA* 5′ UTR contained only 10 nt (known IREs are approximately 30 nt in length); therefore, the *pgdA* 3′ UTR was chosen for further

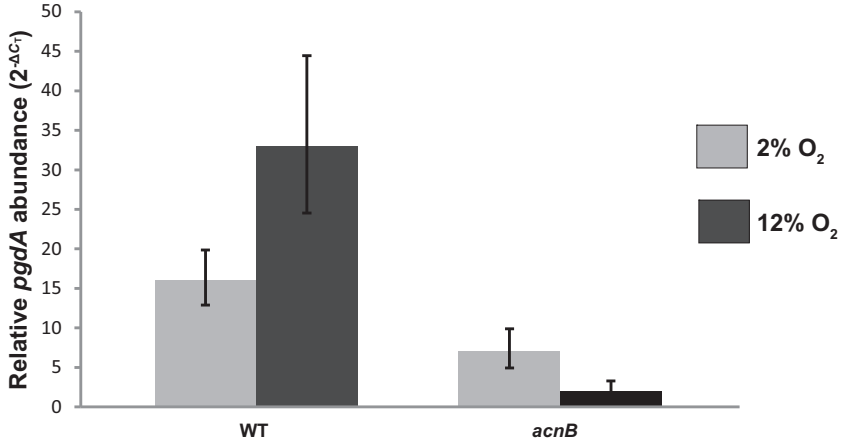

FIG 2 Relative *pgdA* transcript abundance. Transcript levels were determined by quantitative real-time PCR after growth of each strain under either 2 or 12% O_2. The *gyrA* housekeeping gene was used as an internal control. Results shown are representative data from one experiment performed in triplicate. The entire experiment was repeated with similar results. Error bars represent $2^{-(\Delta CT - SD)} - 2^{-\Delta CT}$ and $2^{-\Delta CT} - 2^{-(\Delta CT + SD)}$.

investigation. The secondary structure of the 3′ UTR was predicted using the STAR program (25) (see Fig. 4B), revealing two stem-loops that may be involved in aconitase binding. To test if apo-AcnB could bind to the transcript, electrophoretic mobility shift assays were performed. Radiolabeled *pgdA* probe (50 nM) was incubated with 0, 600, 1,200, and 3,000 nM apo-AcnB protein. As apo-AcnB concentration increased, more *pgdA* probe was observed to shift (Fig. 3A). The addition of ammonium iron (II) sulfate and dithiothreitol resulted in no shift, while the addition of dipyridyl promoted binding (Fig. 3B). These results agreed with other bacterial studies (18, 26) that demonstrated the RNA-binding ability of aconitase is di-

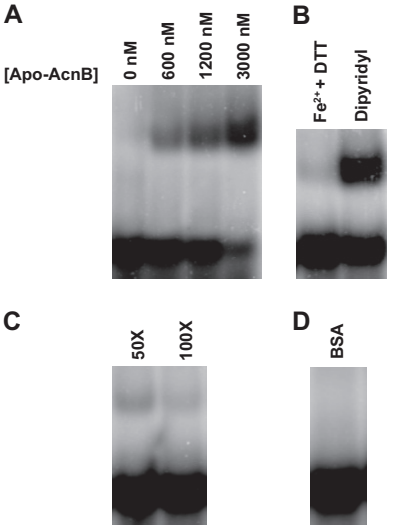

FIG 3 Electrophoretic mobility shift assays. (A) More *pgdA* transcript (50 nM) bound to apo-AcnB with increasing protein concentration. (B) Addition of iron and reductant abolished binding, whereas the iron chelator dipyridyl promoted binding. DTT, dithiothreitol. (C) Radiolabeled *pgdA* probe was outcompeted by specific unlabeled competitor RNA at 100× molar excess. (D) Use of nonspecific protein bovine serum albumin (3,000 nM) instead of apo-AcnB did not result in a shift.

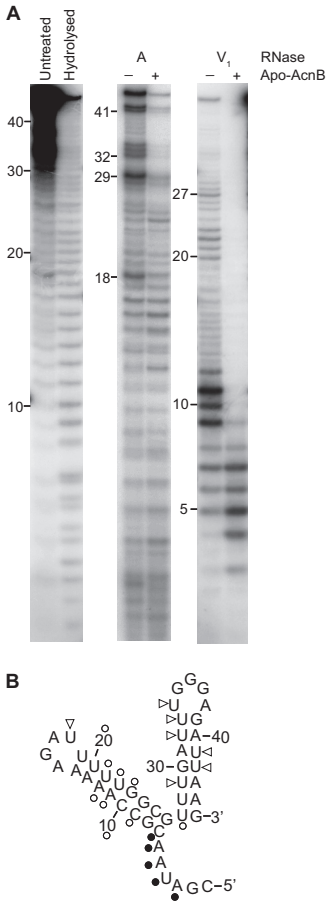

FIG 4 RNA footprinting. (A) 5′-End-labeled 45-nt *pgdA* RNA was incubated with (+) and without (−) apo-AcnB and subjected to RNase digestion. (B) RNase A (triangles) and RNase V_1 (circles) cleavage sites were mapped on the predicted *pgdA* 3′ UTR structure. Open symbols indicate nucleotides that were more protected from RNase cleavage in the presence of apo-AcnB, whereas filled symbols indicate those nucleotides that were less protected.

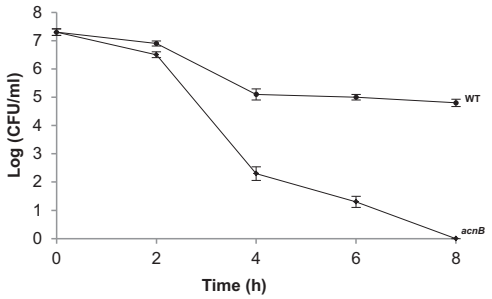

FIG 5 Susceptibility of strains to lysozyme killing. Strains were treated with 50 mg/ml lysozyme, and samples were taken over an 8-h period for comparative viability (CFU determination). Each data point represents averages of combined replicates from two independent experiments (each performed in triplicate). Error bars represent standard deviations. The mutant strain values are significantly lower than the wild-type values at the 4-, 6-, and 8-h time points at $P < 0.01$ (Student's *t* test).

minished upon the addition of Fe^{2+} and restored when iron is not present or the specific iron chelator dipyridyl is added to the reaction. The presence of the [4Fe-4S] cluster in aconitase determines whether it can bind to RNA transcripts (12). Additionally, binding reactions were performed using 50 and 100× molar excesses of specific cold competitor (Fig. 3C). The radiolabeled *pgdA* probe is effectively outcompeted when unlabeled *pgdA* 3′ UTR is added at 100× molar excess. When bovine serum albumin, rather than apo-AcnB, was incubated with the radiolabeled *pgdA* probe, no shift was observed (Fig. 3D). Furthermore, binding reactions were conducted with apo-AcnB (3,000 nM) using a vector-only probe as a negative control, which did not result in a shift, and with the human ferritin IRE as a positive control, which resulted in a shift similar to that of *pgdA* (data not shown).

RNA footprinting was conducted to elucidate where apo-AcnB (dipyridyl treated; see Materials and Methods) was binding to the *pgdA* 3′ UTR. 5′ End-labeled *pgdA* probe was incubated with and without apo-AcnB and subjected to cleavage using two different RNase enzymes (Fig. 4A). RNase A cleaves the 3′ end of single-stranded C and U residues, and RNase V_1 cleaves base-paired or stacked nucleotides. RNase A cleavage of nucleotides 18, 29, 32 to 34, and 41 and 42 occurred less frequently in the presence of apo-AcnB. Incubation with RNase V_1 revealed that the majority of the *pgdA* probe is protected when incubated with apo-AcnB, especially nucleotides 9 to 12, 20 to 23, and 27 (Fig. 4B). Nucleotides 3 to 7 were cleaved more frequently by RNase V_1 in the presence of apo-AcnB.

Deletion of *acnB* confers lysozyme sensitivity in *H. pylori* mutants. Lysozyme hydrolyzes the β-1,4 bonds connecting GlcNAc and MurNAc residues in bacterial PG, leading to decreased cell wall integrity and subsequent cell lysis. Previously, our laboratory showed that an *H. pylori pgdA* strain is more sensitive to lysozyme degradation than the wild type (10). Thus far, our findings suggested apo-AcnB regulates PgdA expression. Therefore, we speculated that the *acnB* strain was more sensitive to lysozyme killing, and this sensitivity was tested over an 8-h period (Fig. 5). The *acnB* strain is significantly more sensitive to lysozyme killing than the wild type after 4, 6, and 8 h ($P < 0.01$), as determined by Student's *t* test. The kill curve for the *acnB* strain closely resembles that previously published for the *pgdA* strain (10).

The *acnB* strain has an attenuated ability to colonize the mouse stomach. We wanted to characterize the physiological role of aconitase in *H. pylori* by comparing the colonization abilities of the *acnB* strain to that of the wild type. Each strain was individually inoculated into eight C57BL/6J mice, and after 3 weeks, stomach colonization was examined. The mean colonization for the wild type was 2.1×10^6 CFU/g, whereas the mean for the *acnB* strain was 4.6×10^5 CFU/g (Fig. 6). Thus, there was a 4.5-fold decrease in mouse colonization by the *acnB* strain. Using the Wilcoxon signed-rank test, the range of mutant colonization values is significantly smaller than that of the wild type at greater than 95% confidence ($P < 0.05$). These results demonstrate aconitase contributes to *H. pylori* survival and colonization in the mouse stomach.

DISCUSSION

During *H. pylori* colonization, host immune cells mount a strong inflammatory response resulting in the production of large amounts of ROS, including hydrogen peroxide (H_2O_2) and the superoxide anion (O_2^-). These can be detrimental to *H. pylori*, causing damage to DNA, proteins, and lipids. Despite containing a diverse repertoire of antioxidant enzymes (3), the bacterium lacks homologues of the oxidative stress response regulators found in other bacteria, such as OxyR, SoxRS, and the RpoS sigma factor. Thus, it has been hypothesized that posttranscriptional regulation in *H. pylori* plays a role in the regulation of genes in

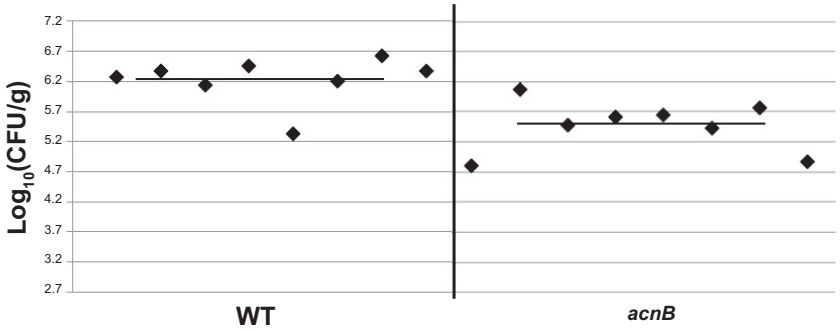

FIG 6 Mouse colonization by strains. Wild-type and *acnB* strains were separately injected into 8 mice each, and colonization ability (CFU recovered per gram of stomach) was examined after 3 weeks. Each point represents the CFU count from one stomach, and solid horizontal lines represent the means of colonization for each strain. The baseline ($\log_{10}$[CFU/g] = 2.7) is the limit of detection. The experiment was repeated with similar results.

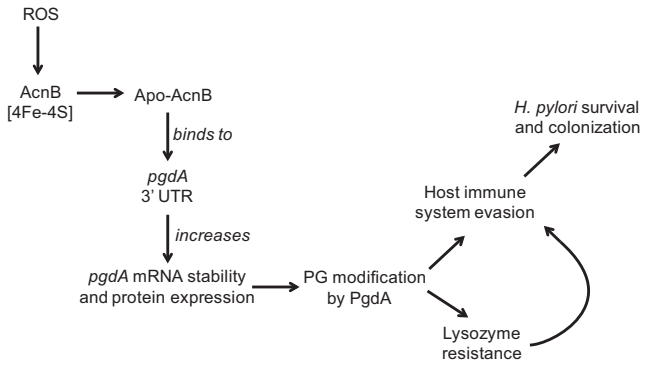

FIG 7 Model of *pgdA* posttranscriptional regulation and its effects on *H. pylori*. ROS oxidize the [4Fe-4S] cluster of AcnB, rendering apo-AcnB, which then binds to the *pgdA* transcript. Increased transcript stability leads to increased expression of the PG-modifying enzyme, PgdA. PG modification is a mechanism *H. pylori* utilizes to circumvent host immune system detection and resist lysozyme degradation (which further mitigates host immune system recognition), both of which contribute to long-term survival and colonization.

response to stress (27). We propose a model for the role of aconitase in *H. pylori* colonization (Fig. 7). Bacterial aconitases are subject to oxidation and Fe/S cluster loss, but the apo-form can still play regulatory roles (16, 18). PgdA has been shown to be upregulated in response to oxidative stress and upon contact with neutrophils (10, 28). Failure of the *acnB* strain to upregulate PgdA expression under 12% O_2 conditions is in contrast to the wild type, and it led us to hypothesize aconitase was playing a role in deacetylase regulation (Fig. 1). Decreased transcript abundance and *pgdA* mRNA half-life in the *acnB* strain supported our hypothesis that aconitase is involved in the posttranscriptional regulation of *pgdA*. Electrophoretic mobility shift assays and RNA footprinting data demonstrated that the regulatory effect of aconitase results from direct interaction between apo-AcnB and the transcript. Furthermore, the *acnB* strain was more sensitive to lysozyme degradation and was attenuated in its ability to colonize the mouse stomach, so an AcnB role *in vivo* is proposed (Fig. 7).

Aconitase-mediated transcript stabilization is a previously described regulatory mechanism. In vertebrates, IRP1 binds to IREs involved in maintaining iron homeostasis (12). The consensus IRE has a C bulge in the stem and the sequence CAGUGN in the loop (12), but the precise structure or sequence recognized by bifunctional bacterial aconitases is less defined. Some aconitase transcript targets contain the eukaryotic consensus sequence, such as thioredoxin (*trxC*) in *M. tuberculosis* (18); however, the *E. coli acnA*, *acnB*, *sodA*, and *ftsH* transcripts as well as the *B. subtilis gerE* transcript do not have the consensus sequence (15–17, 29). The *pgdA* 3′ UTR also does not contain this consensus sequence, but gel shift data indicate binding to apo-AcnB (Fig. 3). RNA footprinting revealed which nucleotides of the *pgdA* 3′ UTR were protected by apo-AcnB (Fig. 4), but it is still unclear which specific nucleotides or sequences are necessary for binding. This appears to be the case for other bacterial aconitase targets as well (16). It is of interest to learn the total repertoire of mRNA targets and the complete role of this tricarboxylic acid (TCA) cycle enzyme.

ACKNOWLEDGMENTS

We thank Bijoy Mohanty for all of his guidance and expertise with the RNA footprinting experiments. We also thank Stéphane Benoit for many helpful discussions and Sue Maier for her help with the mouse colonization experiments.

REFERENCES

1. **Dunn BE, Cohen H, Blaser MJ.** 1997. *Helicobacter pylori*. Clin. Microbiol. Rev. **10:**720–741.
2. **Kusters JG, van Vliet AH, Kuipers EJ.** 2006. Pathogenesis of *Helicobacter pylori* infection. Clin. Microbiol. Rev. **19:**449–490.
3. **Wang G, Alamuri P, Maier RJ.** 2006. The diverse antioxidant systems of *Helicobacter pylori*. Mol. Microbiol. **61:**847–860.
4. **Wang G, Lo LF, Forsberg LS, Maier RJ.** 2012. *Helicobacter pylori* peptidoglycan modifications confer lysozyme resistance and contribute to survival in the host. mBio **3:**e00409–12. doi:10.1128/mBio.00409-12.
5. **Costa K, Bacher G, Allmaier G, Dominguez-Bello MG, Engstrand L, Falk P, de Pedro MA, Garcia-del Portillo F.** 1999. The morphological transition of *Helicobacter pylori* cells from spiral to coccoid is preceded by a substantial modification of the cell wall. J. Bacteriol. **181:**3710–3715.
6. **Mobley HLT, Mendz GL, Hazell SL.** 2001. *Helicobacter pylori*: physiology and genetics. ASM Press, Washington, DC.
7. **Cole AM, Liao HI, Stuchlik O, Tilan J, Pohl J, Ganz T.** 2002. Cationic polypeptides are required for antibacterial activity of human airway fluid. J. Immunol. **169:**6985–6991.
8. **Dziarski R.** 2003. Recognition of bacterial peptidoglycan by the innate immune system. Cell. Mol. Life Sci. **60:**1793–1804.
9. **Davis KM, Weiser JN.** 2011. Modifications to the peptidoglycan backbone help bacteria to establish infection. Infect. Immun. **79:**562–570.
10. **Wang G, Olczak A, Forsberg LS, Maier RJ.** 2009. Oxidative stress-induced peptidoglycan deacetylase in *Helicobacter pylori*. J. Biol. Chem. **284:**6790–6800.
11. **Wang G, Maier SE, Lo LF, Maier G, Dosi S, Maier RJ.** 2010. Peptidoglycan deacetylation in *Helicobacter pylori* contributes to bacterial survival by mitigating host immune responses. Infect. Immun. **78:**4660–4666.
12. **Beinert H, Kennedy MC, Stout CD.** 1996. Aconitase as iron-sulfur protein, enzyme, and iron-regulatory protein. Chem. Rev. **96:**2335–2374.
13. **Dupuy J, Volbeda A, Carpentier P, Darnault C, Moulis JM, Fontecilla-Camps JC.** 2006. Crystal structure of human iron regulatory protein 1 as cytosolic aconitase. Structure **14:**129–139.
14. **Hentze MW, Kuhn LC.** 1996. Molecular control of vertebrate iron metabolism: mRNA-based regulatory circuits operated by iron, nitric oxide, and oxidative stress. Proc. Natl. Acad. Sci. U. S. A. **93:**8175–8182.
15. **Tang Y, Quail MA, Artymiuk PJ, Guest JR, Green J.** 2002. *Escherichia coli* aconitases and oxidative stress: post-transcriptional regulation of *sodA* expression. Microbiology **148:**1027–1037.
16. **Tang Y, Guest JR, Artymiuk PJ, Read RC, Green J.** 2004. Post-transcriptional regulation of bacterial motility by aconitase proteins. Mol. Microbiol. **51:**1817–1826.
17. **Serio AW, Pechter KB, Sonenshein AL.** 2006. *Bacillus subtilis* aconitase is required for efficient late-sporulation gene expression. J. Bacteriol. **188:**6396–6405.
18. **Banerjee S, Nandyala AK, Raviprasad P, Ahmed N, Hasnain SE.** 2007. Iron-dependent RNA-binding activity of *Mycobacterium tuberculosis* aconitase. J. Bacteriol. **189:**4046–4052.
19. **Pitson SM, Mendz GL, Srinivasan S, Hazell SL.** 1999. The tricarboxylic acid cycle of *Helicobacter pylori*. Eur. J. Biochem. **260:**258–267.
20. **Sharma CM, Hoffmann S, Darfeuille F, Reignier J, Findeiss S, Sittka A, Chabas S, Reiche K, Hackermuller J, Reinhardt R, Stadler PF, Vogel J.** 2010. The primary transcriptome of the major human pathogen *Helicobacter pylori*. Nature **464:**250–255.
21. **Wang G, Lo LF, Maier RJ.** 2011. The RecRO pathway of DNA recombinational repair in *Helicobacter pylori* and its role in bacterial survival in the host. DNA Repair (Amsterdam) **10:**373–379.
22. **Benoit SL, Maier RJ.** 2011. Mua (HP0868) is a nickel-binding protein that modulates urease activity in *Helicobacter pylori*. mBio **2**(2):e00039-11. doi:10.1128/mBio.00039-11.
23. **Livak KJ, Schmittgen TD.** 2001. Analysis of relative gene expression data using real-time quantitative PCR and the $2^{-\Delta\Delta CT}$ method. Methods **25:**402–408.
24. **Ysla RM, Wilson GM, Brewer G.** 2008. Chapter 3. Assays of adenylate

uridylate-rich element-mediated mRNA decay in cells. Methods Enzymol. **449:**47–71.
25. **Abrahams JP, van den Berg M, van Batenburg E, Pleij C.** 1990. Prediction of RNA secondary structure, including pseudoknotting, by computer simulation. Nucleic Acids Res. **18:**3035–3044.
26. **Alen C, Sonenshein AL.** 1999. *Bacillus subtilis* aconitase is an RNA-binding protein. Proc. Natl. Acad. Sci. U. S. A. **96:**10412–10417.
27. **Barnard FM, Loughlin MF, Fainberg HP, Messenger MP, Ussery DW, Williams P, Jenks PJ.** 2004. Global regulation of virulence and the stress response by CsrA in the highly adapted human gastric pathogen *Helicobacter pylori*. Mol. Microbiol. **51:**15–32.
28. **Fittipaldi N, Sekizaki T, Takamatsu D, de la Cruz Dominguez-Punaro M, Harel J, Bui NK, Vollmer W, Gottschalk M.** 2008. Significant contribution of the *pgdA* gene to the virulence of *Streptococcus suis*. Mol. Microbiol. **70:**1120–1135.
29. **Tang Y, Guest JR.** 1999. Direct evidence for mRNA binding and post-transcriptional regulation by *Escherichia coli* aconitases. Microbiology **145:**3069–3079.